

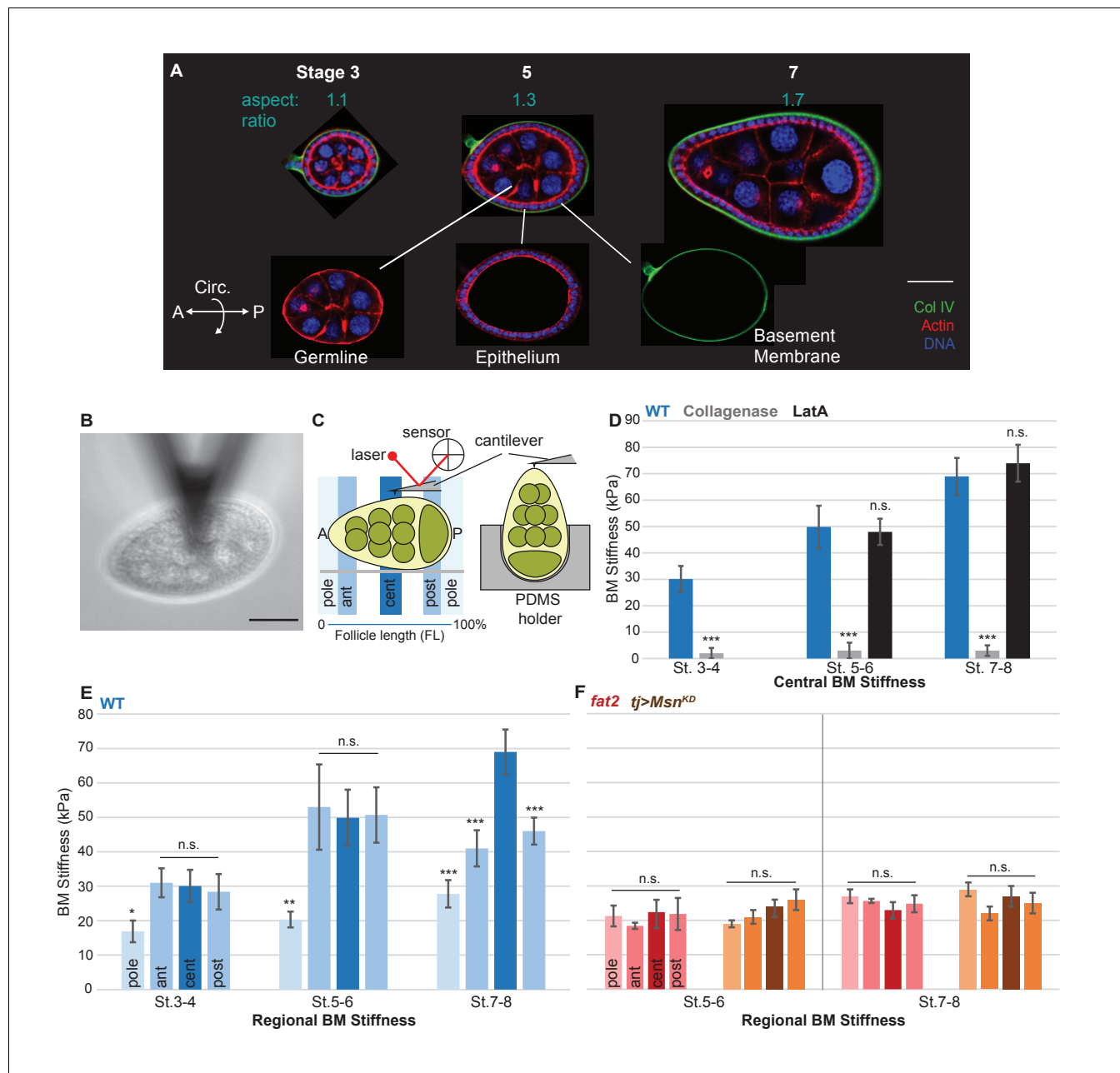


---

## Figures and figure supplements

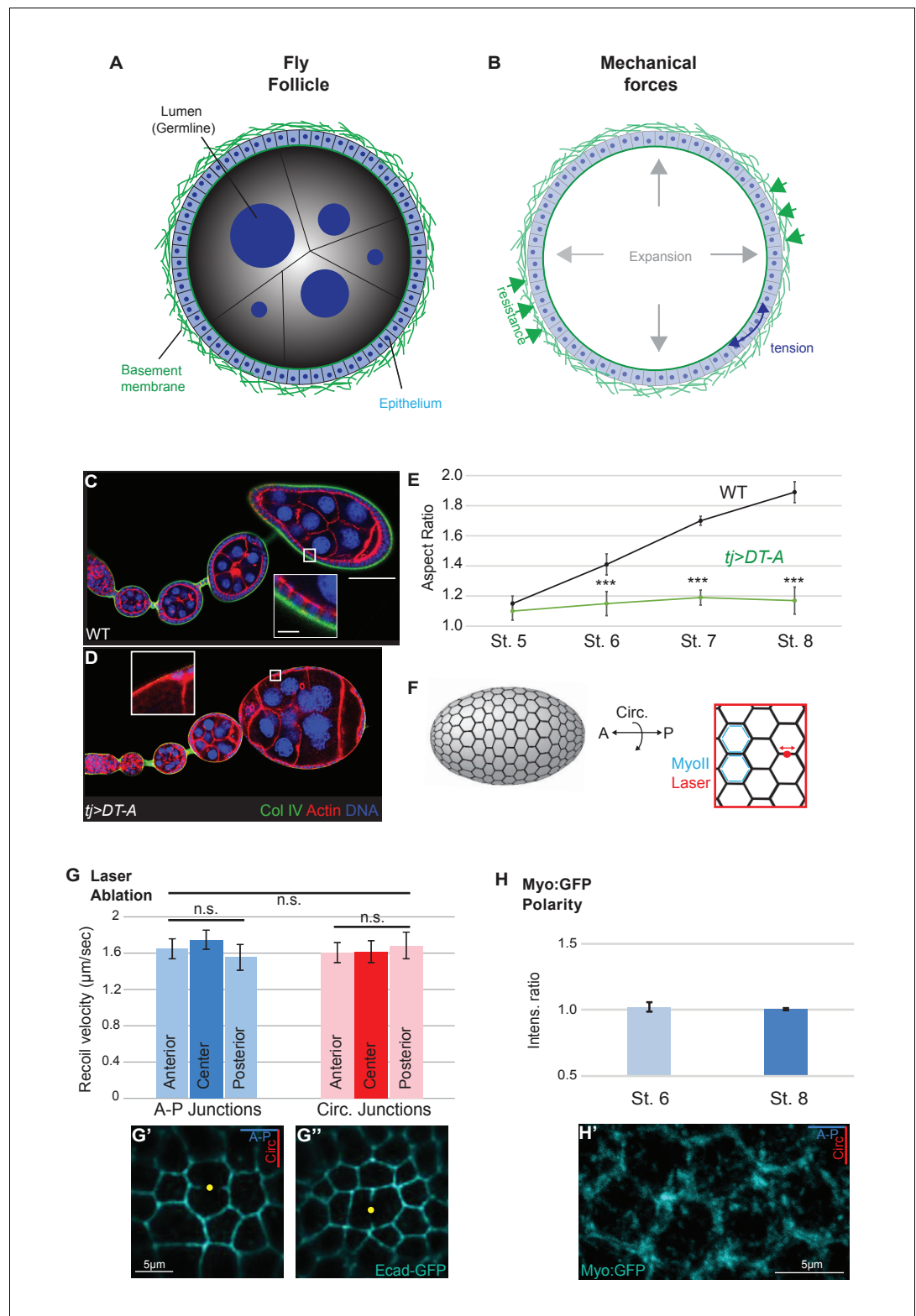
Organ sculpting by patterned extracellular matrix stiffness

**Justin Crest *et al***



**Figure 1.** A mechanical stiffness gradient in the follicle basement membrane. (A) Elongation of the *Drosophila* follicle during oogenesis involves three components: the luminal germline, a surrounding epithelium, and an encasing basement membrane (BM) (see also **Figure 1—figure supplement 1**). Aspect ratios of stage 3, 5, and 7 egg chambers stained for DAPI (blue) and phalloidin (red), along with ColIV-GFP (green), are shown. (B) Atomic Force Microscopy (AFM) measurement of BM stiffness in living follicles. Absence of stroma and external position of BM allow direct access of the AFM probe. (C) Follicles are probed at different regions along the A–P axis, including the poles via Polydimethylsiloxane (PDMS) ‘egg cartons’. Stiffness measurements are derived from the first 50 nm of force–extension curves. (D) BM stiffness in the follicle center increases during development. Collagen digestion but not F-actin network disruption eliminates nearly all AFM-measured stiffness. (cf **Figure 1—figure supplement 1**). (E) Regional BM stiffness along the follicle A–P axis; color intensity matches position as in (C). WT follicles develop an A–P symmetrical gradient of mechanical anisotropy. Anterior and posterior poles are not distinguished. (F) *fat2*- and *msn*-depleted follicle BMs do not increase stiffness during development and remain mechanically isotropic. Scale bar: 25  $\mu$ m.

DOI: [10.7554/eLife.24958.003](https://doi.org/10.7554/eLife.24958.003)



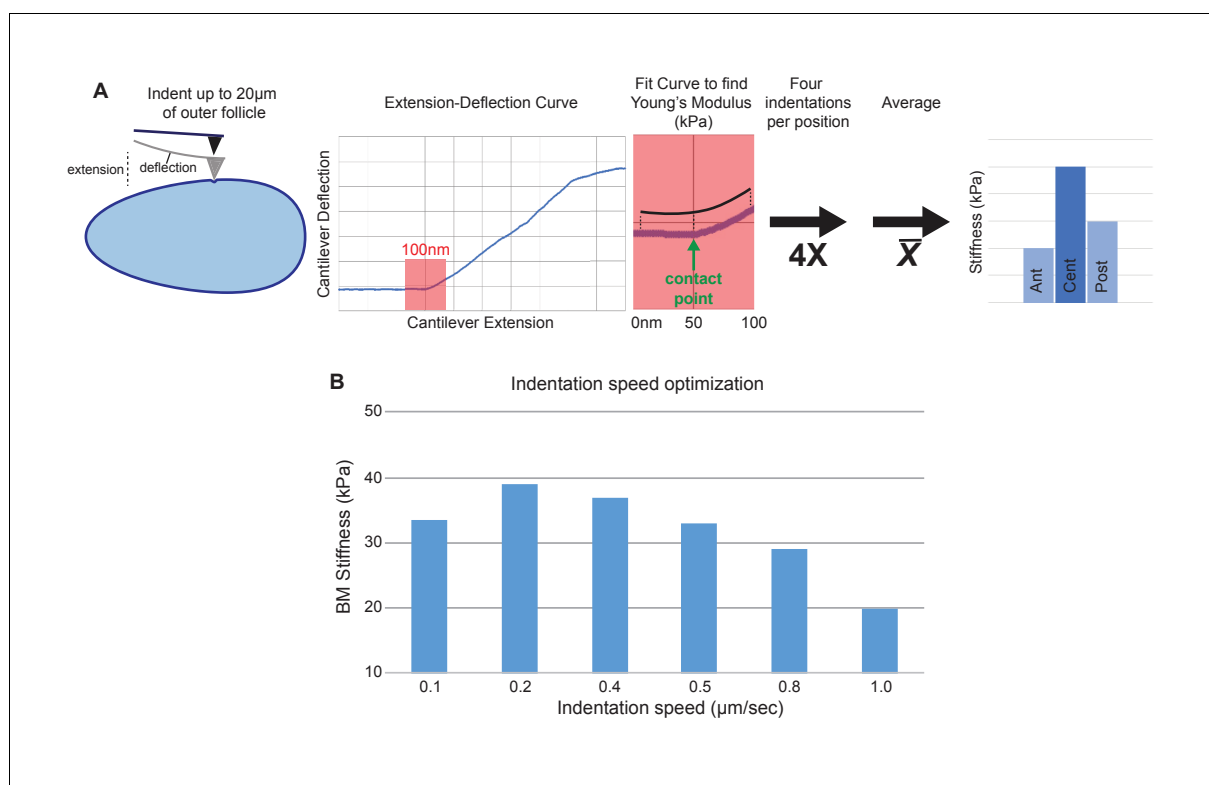
**Figure 1—figure supplement 1.** Isotropic mechanical properties of cells in the *Drosophila* ovary. (A,B) Cross-section of the acinus-like *Drosophila* follicle; planar epithelial and luminal expansionary forces, as well as basement membrane-based resistance, are diagrammed. (C–E) As compared to the elongation of growing WT follicles (C), growth of follicles following ablation of epithelium (*tj*GAL4 *GAL80ts>Diphtheria toxin A chain* [D]) is isotropic. Note the absence of epithelium-produced BM (inset). The aspect ratio is quantitated in (E). (F) Assessment of cortical

Figure 1—figure supplement 1 continued on next page

*Figure 1—figure supplement 1 continued*

tension in follicle epithelial cells using laser nanodissection (red) and Myo:GFP localization (blue). (G) Severing of A–P and circumferential cell junctions at anterior, center, and posterior positions results in comparable recoil velocities. Example A–P and circumferential cuts in G' and G'' are shown. (H) Junctional non-muscle MyoII (Myo:GFP) localization is equivalent along A–P and circumferential cell junctions. Representative example in H'. Scale bars: 25  $\mu\text{m}$  in (A–C), 5  $\mu\text{m}$  inset in (G',H').

DOI: [10.7554/eLife.24958.004](https://doi.org/10.7554/eLife.24958.004)



**Figure 1—figure supplement 2.** AFM elasticity measurement method. (A) Follicles are indented to generate extension–deflection curves. Only the first 50 nm of deflection (plus 50 nm pre-contact) are used to fit for the Young's modulus. Four curves are generated per position, averaged, then compared between A–P positions. (B) Indentation piezo (extension) speed optimization. Reduced stiffness at high speeds (0.8–1.0  $\mu\text{m}/\text{s}$ ) are indicative of viscoelasticity. 0.4  $\mu\text{m}/\text{s}$  provided optimal elasticity accuracy and measurement speed.

DOI: [10.7554/eLife.24958.005](https://doi.org/10.7554/eLife.24958.005)

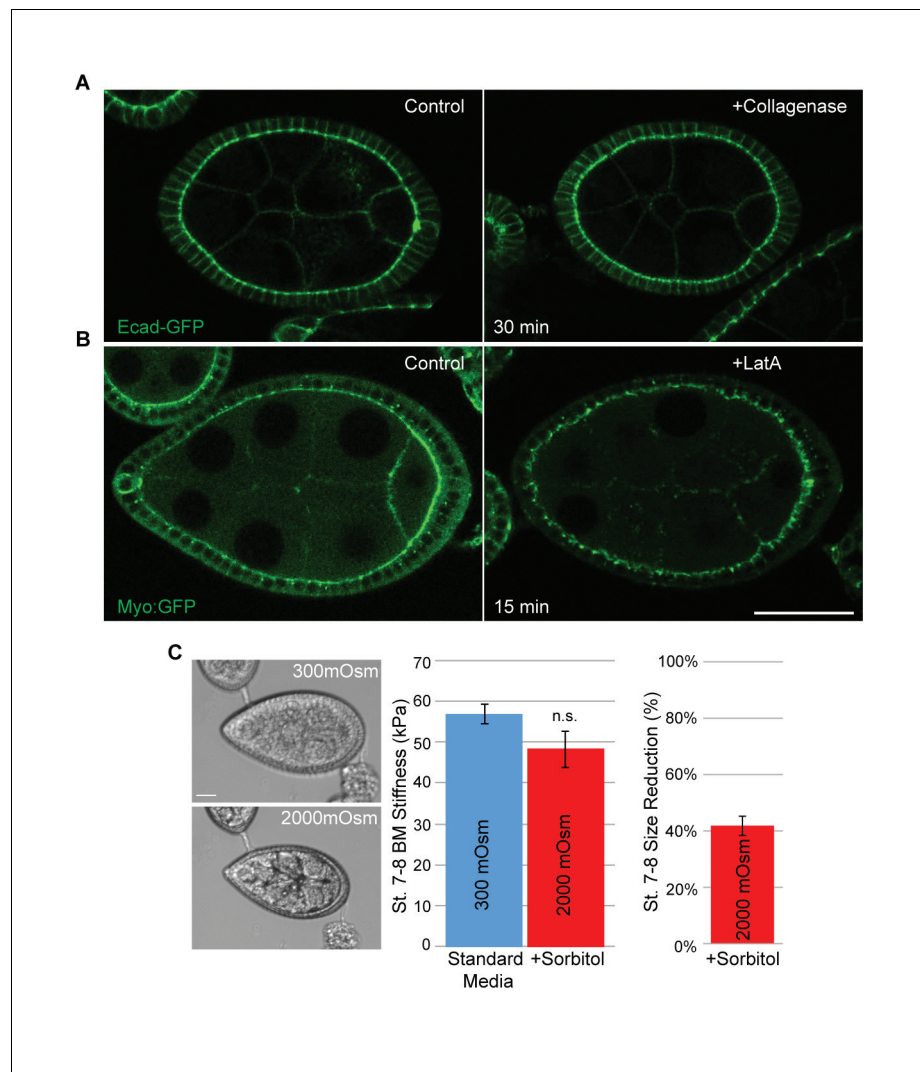


**Figure 1—figure supplement 3.** Validation of pharmacological and hypertonic shock treatments for BM stiffness. (A) Collagenase treatment of follicles prior to AFM does not disrupt cell–cell junctions, as monitored by E-cadherin–GFP. (B) Latrunculin A treatment of follicles prior to AFM effectively displaces Myo:GFP. (C) Hypertonic shrinkage of WT stage 7–8 follicles causes a significant reduction in size, but no significant loss of BM stiffness. Scale bar: 20  $\mu$ m.

DOI: [10.7554/eLife.24958.006](https://doi.org/10.7554/eLife.24958.006)

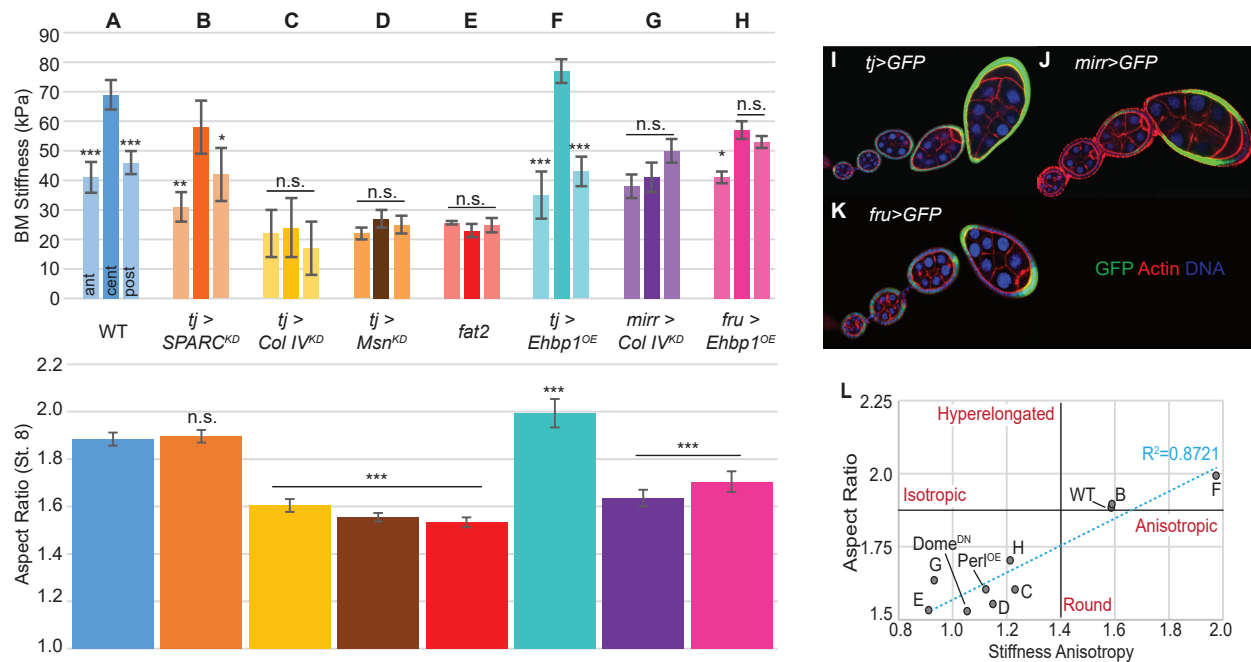


**Figure 2.** Manipulating the BM stiffness gradient alters organ shape. For each follicle genotype, AFM-measured positional stiffness at stages 7–8 is shown above and degree of elongation is shown below. Manipulations in (A–F) alter gene expression uniformly via *tj*GAL4 (I) or homozygous genotype, whereas those in (G, H) alter gene expression regionally using centrally expressed *mir*GAL4 or terminally expressed *fru*GAL4 (J, K). Compared to WT (A), depletion of SPARC (B) softens the BM but preserves the anisotropic gradient; follicles elongate comparably to WT. Depletion of Collagen IV (ColIV) throughout the epithelium (C) creates a uniformly soft follicle with severe elongation defects, resembling mutants in which *msn* is depleted (D) or *fat2* mutants (E). EHBP1 overexpression (F) increases stiffness while retaining an anisotropic gradient, and follicles hyperelongate. Depletion of Col IV in the central region alone (G) flattens the gradient while leaving terminal stiffness intact; this results in elongation defects. EHBP1 overexpression in the terminal regions alone (H) also flattens the gradient and results in elongation defects. (L) Aspect ratio vs stiffness anisotropy (defined as the ratio of central stiffness to the mean stiffness throughout the A–P axis) for genotypes (A–H) and for *tj>Dome<sup>DN</sup>* and *tj>Perl<sup>OE</sup>*.

DOI: 10.7554/eLife.24958.007

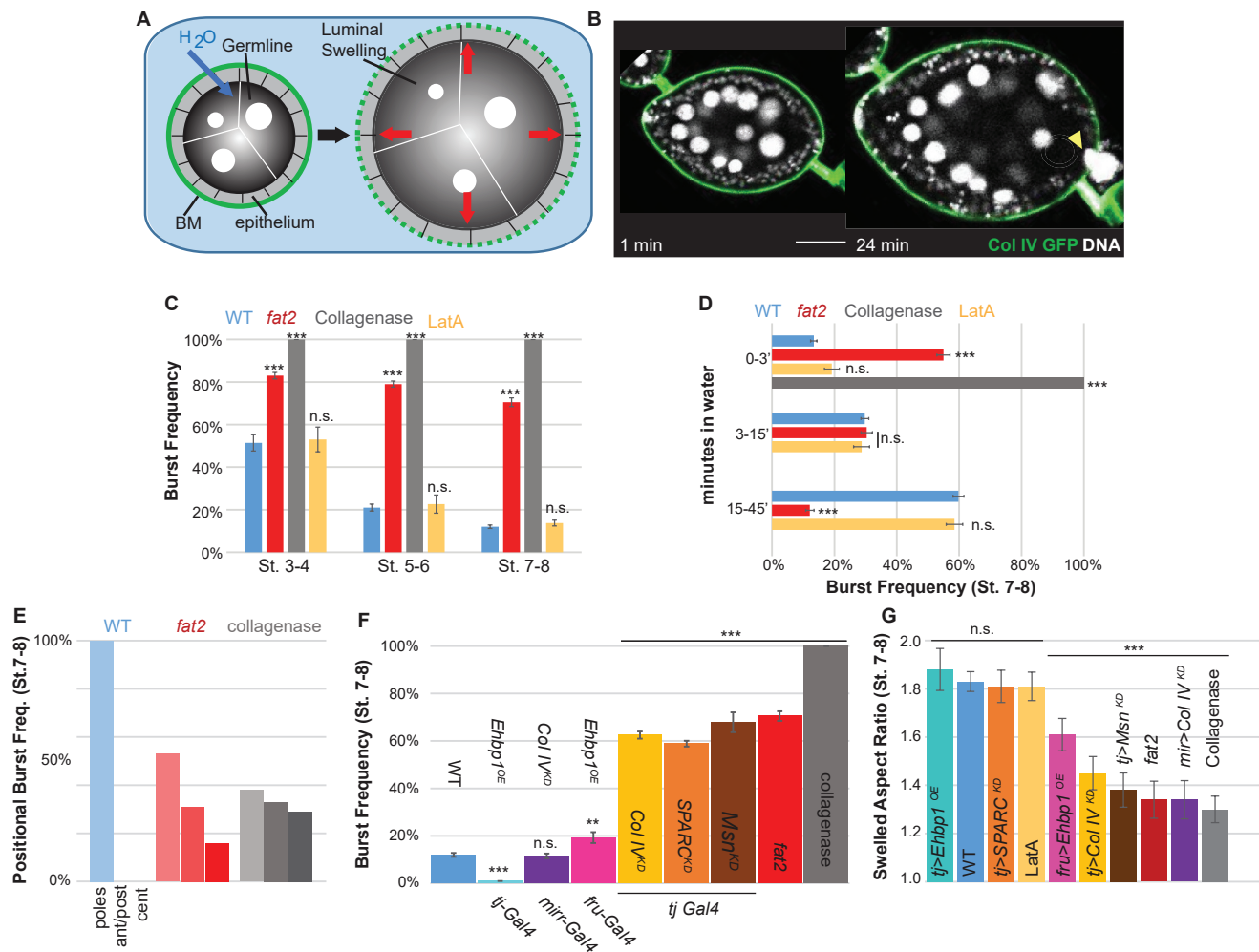


**Figure 3.** The BM stiffness gradient creates anisotropic resistance to organ expansion. (A) Design of osmotic-swelling experiments. Immersion in water causes influx (blue arrow) into the follicle (diagrammed in cross-section), resulting in increased turgor pressure (red arrows) that is resisted by the BM (green) as the organ swells. (B) WT follicle expressing ColIV-GFP, 1 min and 24 min after immersion (cf. **Video 1**). Position of the BM breach is indicated by the yellow arrowhead. (C) Frequency of follicle BM failure by stage and genotype, along with timing (D) of failure. WT BMs accommodate expansion with increasing efficiency as development proceeds in a manner independent of cellular F-actin; *fat2* and collagenased follicles burst frequently and rapidly. (E) Position of BM failure: WT BMs breach most frequently at the poles, whereas *fat2* and collagenased follicles also breach in other regions. (F) Frequency of BM failure in manipulated stage 7–8 follicles and (G) aspect ratio immediately before bursting. Scale bar: 25 μm.

DOI: [10.7554/eLife.24958.011](https://doi.org/10.7554/eLife.24958.011)



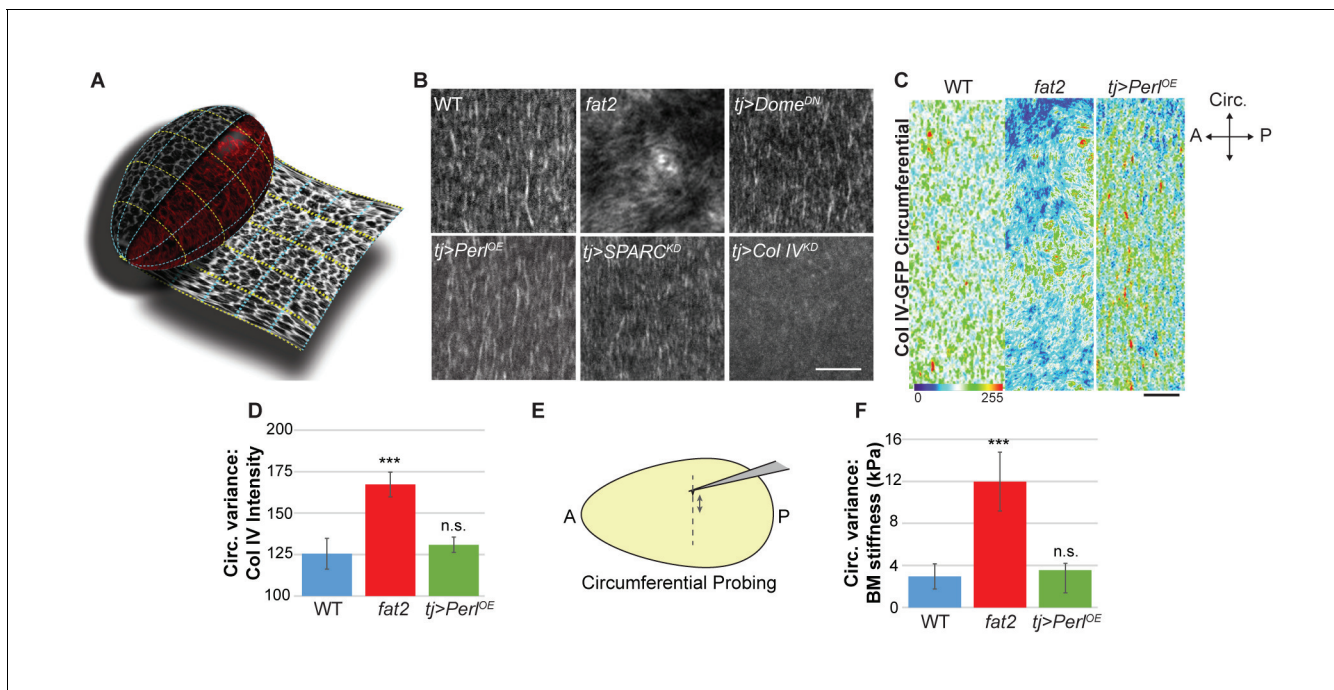


**Figure 4.** Uniform circumferential mechanics in elongating follicles. (A) ‘Unrolling’ of organ surface by ImSAnE allows quantitation of BM components along both A–P and circumferential axes. Image taken from [Chen et al. \(2016\)](#). (B) Analysis of BM fibril PCP shows WT polarity when Perl or Dome<sup>DN</sup> are overexpressed or when SPARC is depleted, contrasting with altered polarity in *fat2* and absence of polarity in Col IV-depleted mutants. (C, D) Unrolling reveals increased variance in circumferential Col IV levels in *fat2* as compared to those in WT or Perl-overexpressing follicles. The heat map indicates lowest (blue) to highest (red) intensities over equivalent ~35% circumferential segments. (E, F) AFM analysis along the circumferential axis of a follicle at a single central meridian. *fat2* mutant follicles show high variability in BM stiffness, compared to the consistent values of WT or Perl-overexpressing follicles. Scale bars: 5  $\mu$ m (B) and 10  $\mu$ m (C).

DOI: [10.7554/eLife.24958.012](https://doi.org/10.7554/eLife.24958.012)

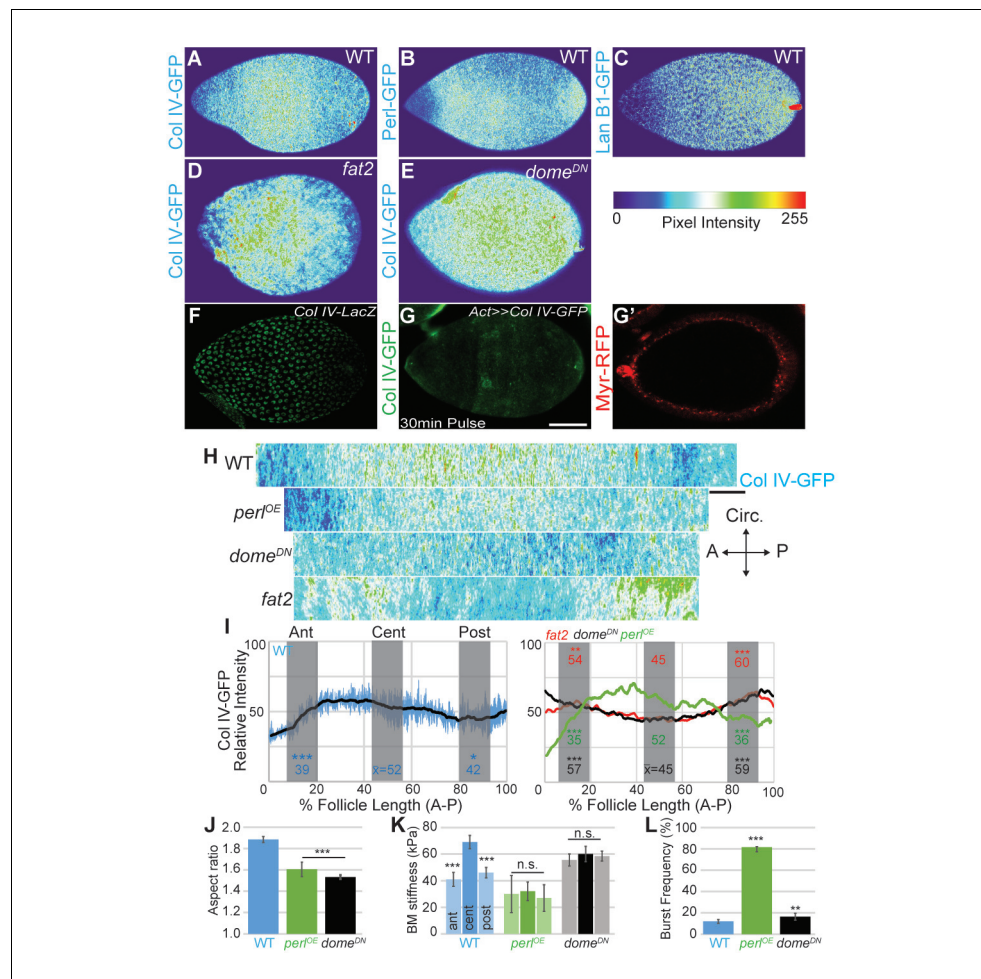


**Figure 5.** Morphogen-like signaling creates the stiffness gradient. Expression of GFP protein traps in BM components, assessed in WT stage 7–8 follicles that are physically flattened for visualization: (A) CollIV, (B) aminin B1, and (C) Perlecan. Heat maps indicate lowest (blue) to highest (red) intensities. The A–P CollIV pattern is disrupted in stage 7–8 follicles mutant for *fat2* ([D], cf. **Figure 5—figure supplement 1**) or with inhibited JAK/STAT signaling (*tj>dome<sup>DN</sup>*, [E]) (cf. **Figure 5—figure supplement 2**). (F) Col IV transcription (*ColIV-LacZ* reporter expression) is not elevated in the central follicle. (G) Uniform production of CollIV (via *hsFLP*; *act>y+>GAL4 UAS-myr-RFP*) throughout the follicle (G') results in elevated central incorporation. (H) ImSAnE 'unrolling' of the CollIV–GFP expressing follicle surface allows quantitation of intensity along the entire A–P axis; note the shorter axis of 'round' genotypes. (I) Along the A–P axis, CollIV levels are significantly elevated in the central region of WT and Perl-overexpressing follicles but not of *fat2* or *dome<sup>DN</sup>*-expressing follicles. (J) Elongation failure is induced by inhibition of JAK-STAT signaling or by overexpression of Perl in follicles. (K) AFM reveals that follicles with inhibited JAK-STAT signaling or Perl overexpression do not develop an A–P stiffness gradient; Perl overexpressing follicles are softer than WT follicles. (L) Perl-overexpressing follicles burst easily under osmotic challenge, whereas follicles with inhibited JAK-STAT signaling are more similar to WT. Scale bars: 25  $\mu$ m (A–G') and 10  $\mu$ m (H).

DOI: 10.7554/eLife.24958.013

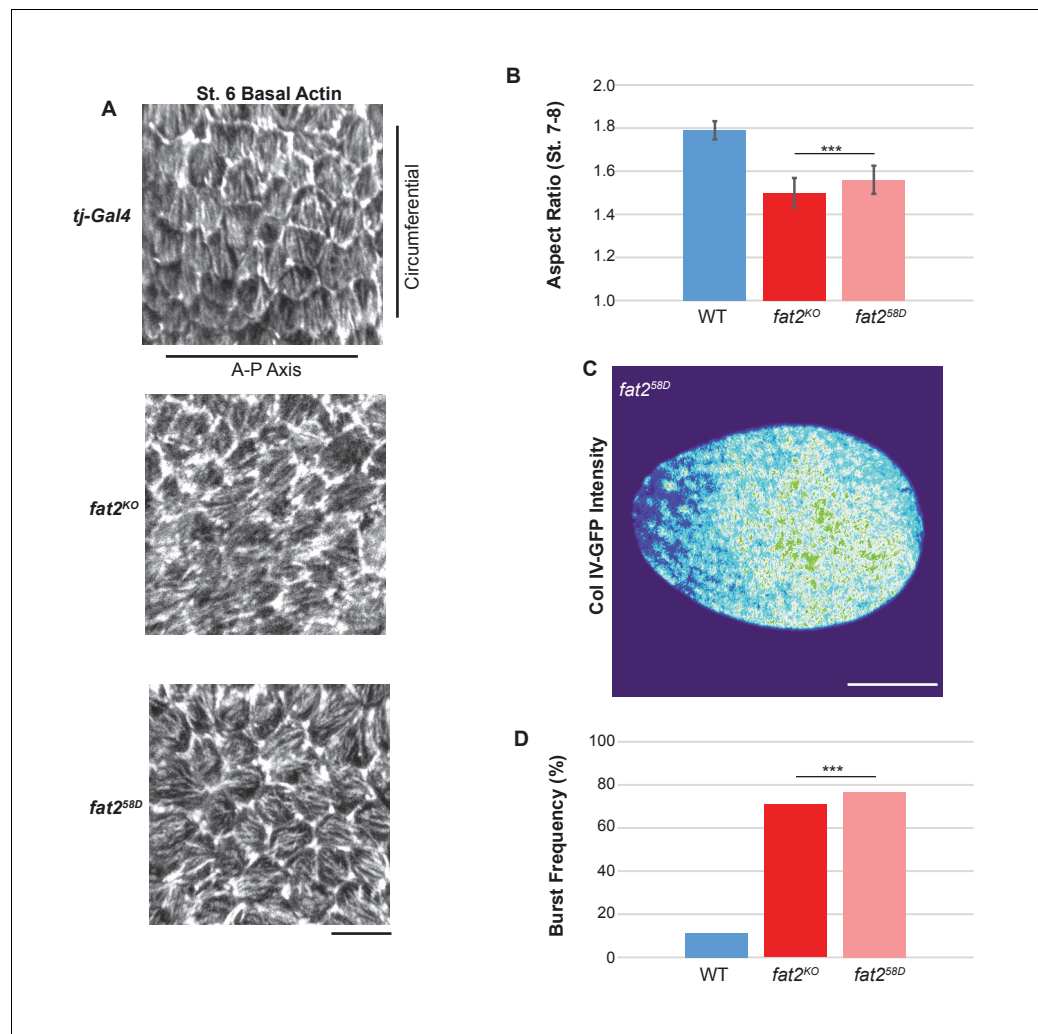


**Figure 5—figure supplement 1.** *fat2<sup>KO</sup>* phenocopies other *fat2* null alleles. (A) Loss of basal actin PCP, (B) elongation defects, (C) Collagen IV–GFP pattern (compare to **Figure 6D**) and (D) bursting frequency in distilled water are indistinguishable between *fat2<sup>KO</sup>* and the well-characterized EMS-generated null allele *fat2<sup>58D</sup>*. Scale bars: 10  $\mu$ m (A) and 20  $\mu$ m (C).

DOI: [10.7554/eLife.24958.014](https://doi.org/10.7554/eLife.24958.014)

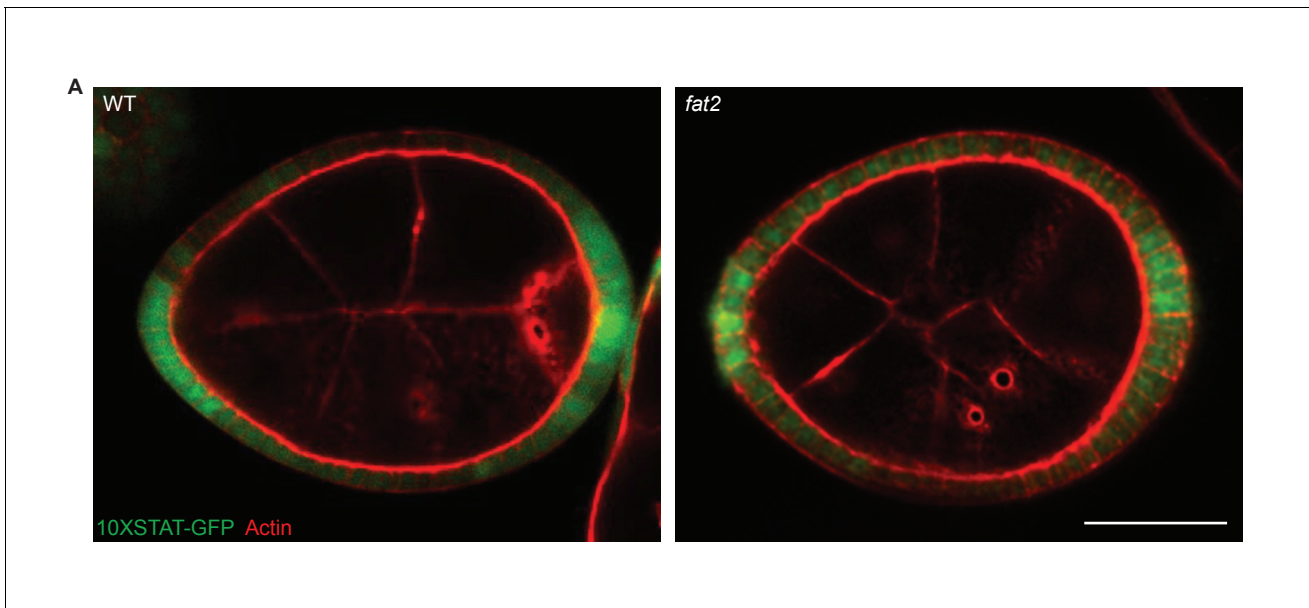


**Figure 5—figure supplement 2.** STAT reporter in *fat2* mutants. (A) *fat2* loss does not disrupt A–P patterning as detected by the 10XSTAT–GFP reporter. Scale bar: 20  $\mu$ m.

DOI: [10.7554/eLife.24958.015](https://doi.org/10.7554/eLife.24958.015)

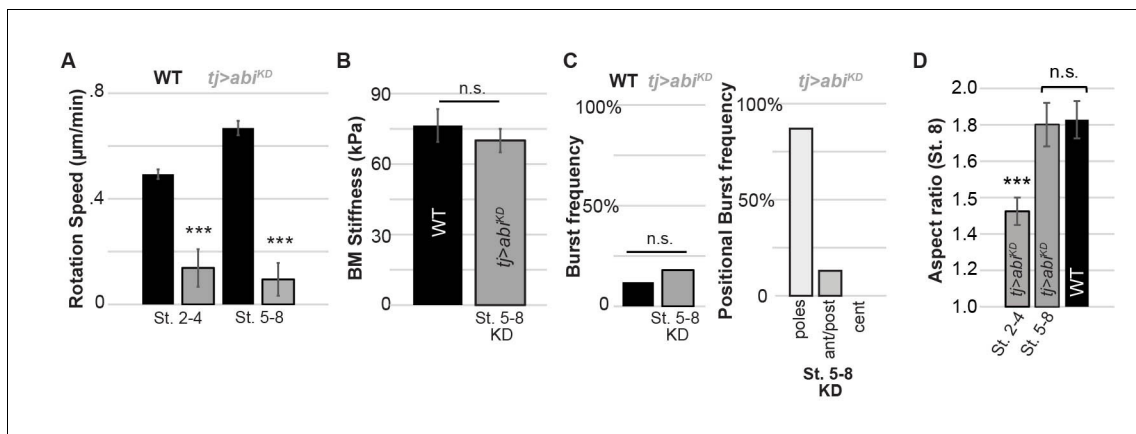


**Figure 5—figure supplement 3.** BM stiffness and active follicle rotation. Depletion of actin regulator Abi following stage 5 (A) halts rotation but (B) does not soften BM at stage 7–8 nor (C) alter bursting characteristics at stage 7–8; (D) follicles show normal elongation at stage 7–8 (cf. **Cetera and Horne-Badovinac, 2015**).

DOI: [10.7554/eLife.24958.016](https://doi.org/10.7554/eLife.24958.016)